Hindawi
Journal of Nanomaterials
Volume 2018, Article ID 2580171, 6 pages
https://doi.org/10.1155/2018/2580171

Research Article

Atomic-Scale Finite Element Method for Analyzing the Sensitivity of Graphyne-Based Resonators

Haw-Long Lee, Yu-Ching Yang, and Win-Jin Chang

Department of Mechanical Engineering, Kun Shan University, Tainan 71003, Taiwan

Correspondence should be addressed to Win-Jin Chang; changwj@mail.ksu.edu.tw

Received 9 May 2018; Revised 16 July 2018; Accepted 24 July 2018; Published 5 August 2018

Academic Editor: Stefano Bellucci

An atomic-scale finite element method was applied to analyze the sensitivities of α-, β-, γ-, and 6,6,12-graphyne-based resonators in mass detection under different boundary conditions. These sensitivities are then compared with that of a graphene-based resonator obtained in a previous study. According to the analysis results, among the graphyne-based resonators, the α type shows the highest sensitivity, while the γ type shows the lowest. In addition, the sensitivity decreases as the resonator size increases. We also find that the location of the attached mass has a significant effect on the sensitivity of the γ-graphyne-based resonators with different attached masses. The α-graphyne-based resonator with a small attached mass is also sensitive to change in location. However, the situation is different for a large attached mass. This study is significant for the future design and application of a graphyne-based resonator with high sensitivity.

1. Introduction

Graphyne, as first proposed by Baughman et al. [1], is constructed by inserting an acetylenic linkage (–C≡C–) between two bonded C atoms of graphene. The presence of acetylenic linkages in graphyne results in unique mechanical, thermal, optical, and electrical properties, which are significantly different from those of graphene [2, 3]. Graphyne exists in four typical geometrical forms—α-graphyne, β-graphyne, γ-graphyne, and 6,6,12-graphyne—due to the various arrangements of acetylenic linkages and their insertion percentages [1]. The percentages of acetylenic linkages for α-graphyne, β-graphyne, 6,6,12-graphyne, γ-graphyne, and graphene are 100%, 66.67%, 41.67%, 33.33%, and 0%, respectively. The structures of four types of graphyne allotropes, as well as that of graphene, are depicted in Figure 1.

Recently, numerous researchers have studied the mechanical, thermal, and electronic properties of graphyne. For example, Cranford and Buehler [4] carried out molecular dynamics simulations to investigate the mechanical properties of single-atomic-layer graphyne sheets and showed that this material has interesting mechanical properties, which differ from those of graphene. In addition, the intersheet adhesion energy and bending stiffness were found to be comparable to those of graphene, while the density of graphyne being only one-half that of graphene. Peng et al. [5] investigated the mechanical properties of graphyne monolayers under various strains and the pressure effects on Young's modulus and Poisson ratio using first-principle calculations based on density functional theory. Ajori et al. [6] explored the mechanical properties of perfect and defective γ-graphyne by using molecular dynamics simulation and found that the vacancy defects reduced Young's modulus and that ultimate stress and strain increased Poisson's ratio. Perkgöz and Sevik [7] studied the vibrational and thermodynamic properties of the graphene-related structures of α-graphyne, β-graphyne, γ-graphyne, and 6,6,12-graphyne by using density functional perturbation theory. Based on that theory, the thermodynamic stability of different graphyne allotropes was assessed by investigating their vibrational properties, lattice thermal expansion coefficients, and Gibbs free energy values.

In addition, Couto and Silvestre [8] evaluated the elastic properties of graphyne by using a finite element model and showed that graphyne exhibits marginal orthotropic behavior. Recently, Qu et al. [9] developed a molecular

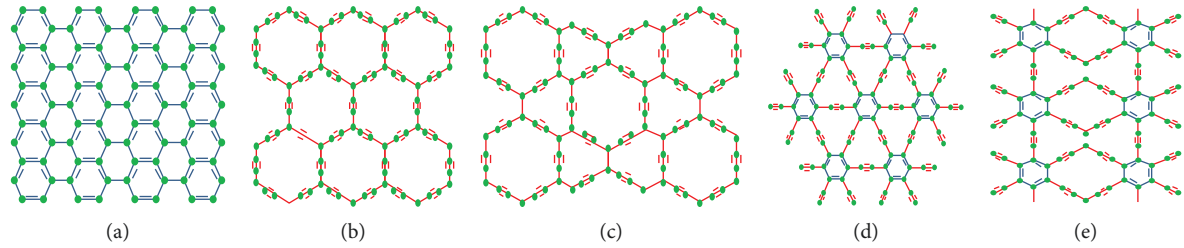

Figure 1: Structures of (a) graphene, (b) α-graphyne, (c) β-graphyne, (d) γ-graphyne, and (e) 6,6,12-graphyne.

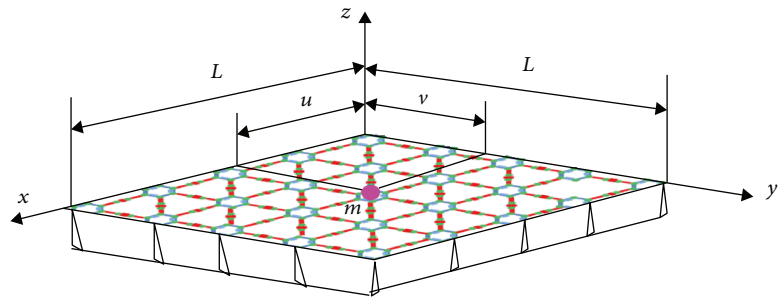

Figure 2: Simply supported graphyne-based resonator with an attached mass.

mechanics model to study the structure-dependent elastic properties of β-graphyne and found that with the increasing length of acetylenic chains, the in-plane stiffness, in-plane shear stiffness, and layer modulus significantly decreased, whereas the Poisson's ratio slightly increased. Rodrigues et al. [10] investigated the nonlinear mechanical behavior of perfect γ-graphyne by using an atomistic finite element model. Bagheri et al. [11] examined the adsorption behavior of a water droplet on graphene and graphyne externals using molecular dynamics simulations and demonstrated that graphyne is more hydrophobic than graphene.

Because performing experiments that accurately characterize and measure the physical properties of graphyne is extremely challenging, theoretical methods, including finite element methods and atomistic simulations, are often used, including those proposed in the previously mentioned studies. However, molecular dynamics simulations are time-consuming [12, 13]. In addition, most of the aforementioned studies have focused on the electronic and mechanical properties of graphyne allotropes, and only a few are available on vibration behavior. In this study, we used an atomic-scale finite element method to investigate the vibrational properties of α-, β-, γ-, and 6,6,12-graphyne-based resonators and examine their sensitivities as a resonator for detecting an attached mass.

2. Atomic-Scale Finite Element Analysis

A simply supported, square graphyne sheet has a length L along the x-axis, width L along the y-axis, and thickness along the z-axis, as shown in Figure 2. The origin is taken at one corner of the midplane of the graphyne sheet, to which a concentrated mass m is attached at an arbitrary location $x = u$ and $y = v$. Here, we calculate the frequency of the graphyne sheet to assess its feasibility for being used as a nanomechanical resonator. An atomic-scale finite element modeling method using commercially available ANSYS FE code was adopted in the frequency analysis. The graphyne sheet can be simulated as a plane-frame structure with beam members, describing their bonds of connecting two nearest-neighbor carbon atoms and joints of the beam elements as atoms in the analysis. A three-dimensional elastic BEAM4 element is used to model the bonds. All parameters used in the calculation are easily determined using the basic formulas $A = \pi d^2/4$ and $I = \pi d^4/64$, where d is the cross-sectional diameter of a bond, A is the cross-sectional area, and I is the moment of inertia. Then, the tensile resistance EA and flexural rigidity EI can also be obtained. Here, E is the Young's modulus of the bond. Based on energy equivalence theory [14], the relation between the force field constants in molecular mechanics and the beam element stiffness in structural mechanics can be developed [15]. In addition, on the basis of structural dynamics theory, the equation of motion of graphyne for the free vibration of an undamped structure is expressed as

$$[M]\{\ddot{z}\} + [K]\{z\} = \{0\}, \quad (1)$$

where $[M]$ and $[K]$ indicate the overall mass and stiffness matrices and $\{z\}$ and $\{\ddot{z}\}$ indicate the nodal displacement vector and acceleration vector, respectively.

For a harmonic vibration, eigenvalues were calculated from the overall stiffness and mass matrices, and fundamental frequencies of graphyne were obtained from the minimum eigenvalues. The resonant frequency is sensitive to the mass attached on the resonator, and the frequencies necessarily shift due to the added mass. Using the overall

mass matrix, the effects of the added masses on the system and frequency shifts Δf are evaluated [15, 16].

In addition, we studied the sensitivity, S, of a graphyne-based resonator, which is defined as the ratio of change in frequency to change in the attached mass, $\Delta f/\Delta m$, and indicates the ability of the resonator to detect the attached mass. For the same attached mass, a larger frequency shift represents higher sensitivity performance of the resonator.

3. Results and Discussion

This study examined the sensitivity of a single-layer graphyne resonator. There are three types (i.e., aromatic, single, and triple) of covalent bonding constructed on the basis of graphyne allotropes. The geometrical and mechanical parameters of the three bonding types used in the analysis have the following values [8]: $d = 1.284$ Å for aromatic and single bonds and $d = 1.954$ Å for a triple bond; $A = 1.0$ Å^2 for aromatic and single bonds and 3.0 Å^2 for a triple bond; $I = 0.07958$ Å^4 for aromatic and single bonds and 0.7162 Å^4 for a triple bond; and $E = 167.616$ nN/Å^2 for an aromatic bond, $E = 166.964$ nN/Å^2 for a single bond, and $E = 25.852$ nN/Å^2 for a triple bond. To our knowledge, this is the first report focused on the vibration sensitivity of graphyne-based resonators. To verify the accuracy of our ANSYS model for calculating vibration response of graphyne membrane, we compare the present result with the previous study. A γ-graphyne membrane with clamped–free–free–free boundary condition was considered in the comparison. The parameters used for the analysis were the same as those used by Couto and Silvestre [8]. The Young's moduli of armchair and zigzag graphyne membranes obtained from the present study were 208.5 and 228.4 N/m, respectively. The results were the same as those obtained by Couto and Silvestre [8]. This comparison was also made in our recently published article [17].

The sensitivities of the graphyne-based resonator differ with different boundary conditions because of their constraints. In the analysis, four boundary conditions are considered: all sides clamped (CCCC), all sides simply supported (SSSS), clamped–free–clamped–free (CFCF), and simply supported–free–simply supported–free (SFSF). The sensitivities of different graphyne and graphene-based resonators were investigated. Figure 3 shows the sensitivities of the α-, β-, γ-, and 6,6,12-graphyne-based resonators under the SSSS boundary condition for $L = 10$ nm and $u = v = L/2$. In addition, the sensitivities of the graphyne-based resonators were compared with those of the graphene-based resonators obtained from the previous study [18]. We observed that the sensitivities of the α-, β-, γ-, and 6,6,12-graphyne-based and graphene-based resonators differed due to the different percentages and mass densities of acetylenic linkages. The sensitivities of the resonator in mass detection were obtained in the following order: α-graphyne > β-graphyne > 6,6,12-graphyne > γ-graphyne > graphene. The same order was observed for the percentages of acetylenic linkages contained in the structure. For different graphyne-based resonators, the discrepancy was more obvious, especially at a small attached mass.

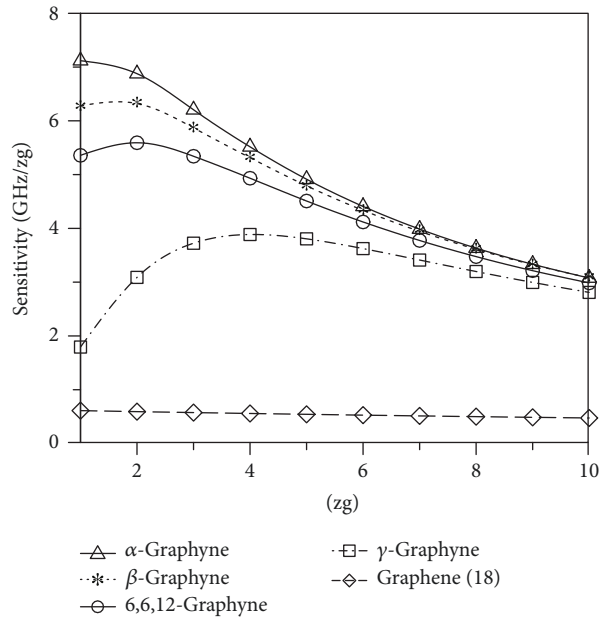

Figure 3: Sensitivity of the α-, β-, γ-, and 6,6,12-graphyne-based and graphene-based resonators under SSSS boundary condition for $L = 10$ nm and $u = v = L/2$.

For the case of an attached mass of 1 zg, the value was 7.1 GHz/zg for the α type and only 1.9 GHz/zg for the γ type. The discrepancy decreased as the attached mass increased. The α type showed considerable sensitivity even at a very small mass, which decreased with an increase in the attached mass. However, the trend was different for the other allotropes. The other types showed a critical point of sensitivity; for example, the γ type showed a critical point of 3.9 GHz/zg corresponding to the attached mass of 4 zg. The sensitivity of the graphene-based resonator was much smaller than those of graphyne-based resonators due to the effect of mass density. The carbon atomic number of graphene is 3984, which is higher than that obtained for graphynes in the analysis, such as 2728 for γ type and 2166 for α type, although the stiffness of graphene is larger than that of graphyne [4].

Figure 4(a) shows the sensitivity of the α-graphyne-based resonator with different attached masses for $L = 10$ nm and $u = v = L/2$ under different boundary conditions. The sensitivity is related to the frequency shift of the resonator with an increase in the attached mass. The sensitivity of the resonator under the CCCC boundary condition was the highest. The sensitivities of the resonator in mass detection were obtained in the following order: CCCC > SSSS > CFCF > SFSF. The sensitivity of the resonator under the CCCC boundary condition was very close to that under the SSSS condition. In addition, the sensitivity was very close under both CFCF and SFSF conditions. However, the discrepancy was large for the γ-graphyne-based resonator under different boundary conditions, as shown in Figure 4(b).

Figure 5(a) shows the size effect on the sensitivity of the α-graphyne-based resonator under the SSSS boundary

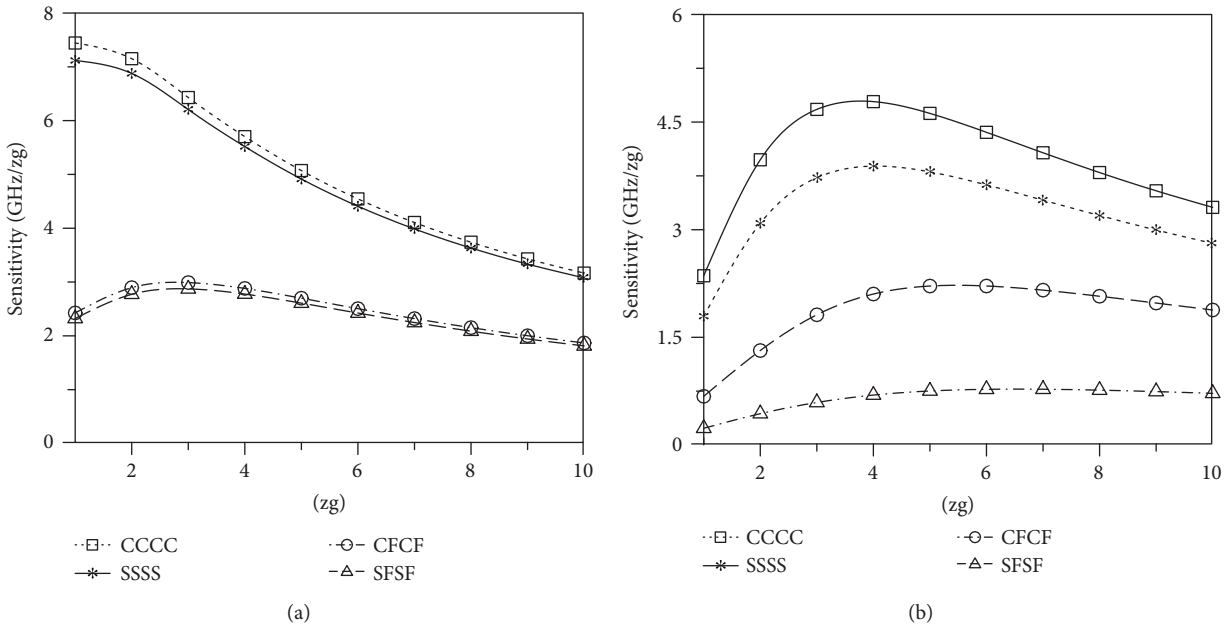

Figure 4: Sensitivity of the (a) α- and (b) γ-graphyne-based resonators with different attached masses for $L = 10$ nm and $u = v = L/2$ and different boundary conditions.

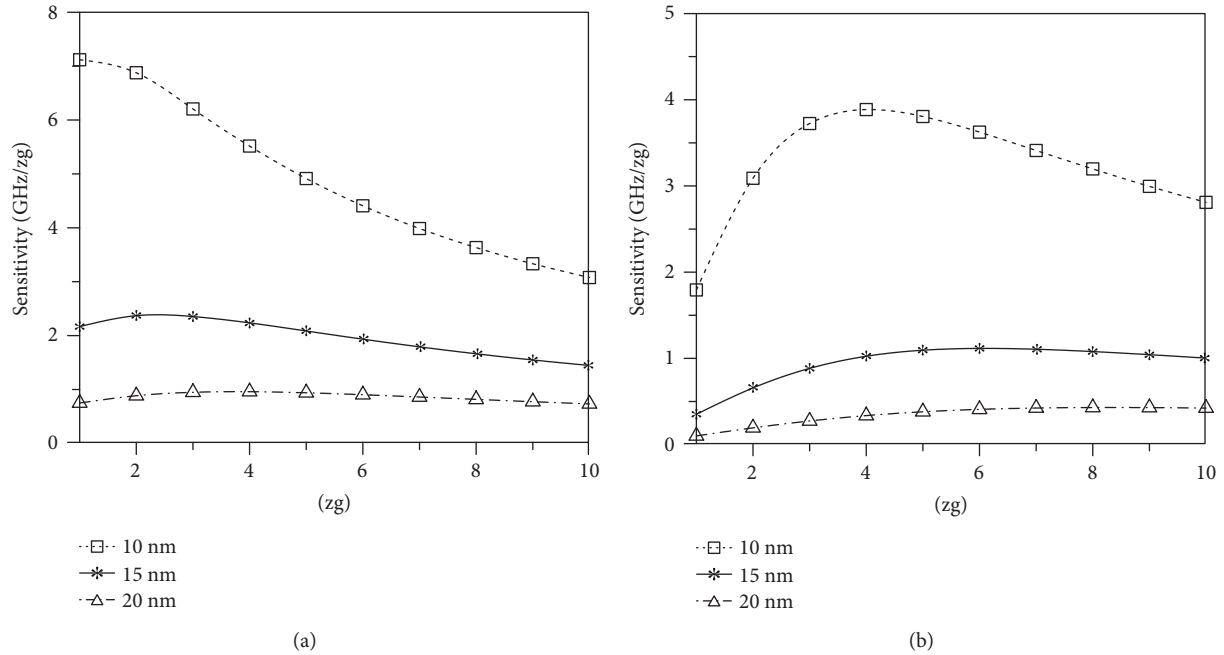

Figure 5: Size effect on the sensitivity of the (a) α- and (b) γ-graphyne-based resonators under SSSS boundary condition for $u = v = L/2$.

condition for $u = v = L/2$. The sensitivity in mass detection decreased with increasing size effect. The same trend was observed for the γ-graphyne-based resonator, as shown in Figure 5(b), because the frequency shift decreased with increasing size and mass of the resonator.

Figure 6(a) illustrates the effect of location of the attached mass on the sensitivity of the α-graphyne-based resonator under SSSS boundary condition for $L = 10$ nm. The sensitivity was the highest when the attached mass was located at the center of the resonator and gradually decreased as the mass moved away from the center. Similar phenomena were obtained for the γ-graphyne-based resonator as shown in Figure 6(b). The effect of location on the sensitivity of the γ-graphyne-based resonator is also clear for detecting a larger mass, but that of the α-graphyne-based resonator is not.

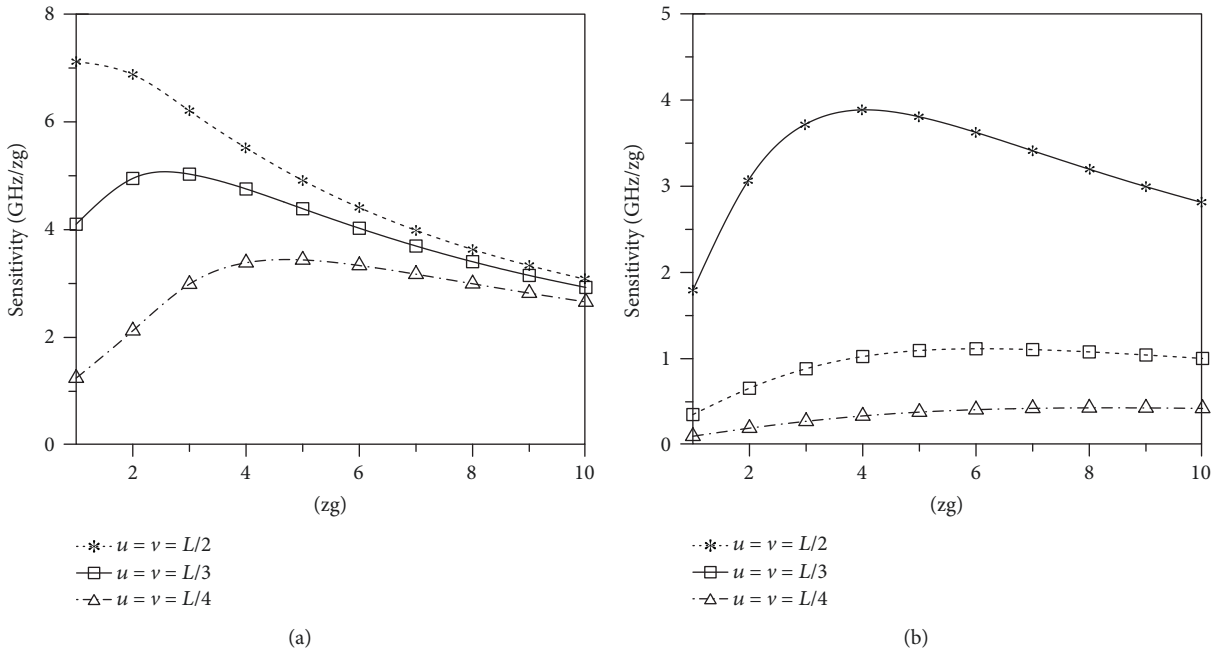

Figure 6: Effect of location of the attached mass on the sensitivity of the (a) α- and (b) γ-graphyne-based resonators under the SSSS boundary condition for $L = 10$ nm.

4. Conclusions

In this study, atomic-scale finite element simulations for α-, β-, γ-, and 6,6,12-graphyne-based resonators under CCCC, SSSS, CFCF, and SFSF boundary conditions were performed using commercially available ANSYS software. The sensitivities of the graphyne-based resonators with various attached masses were studied and compared with that of a graphene-based resonator obtained from a previous study. The analytical results showed that the sensitivities of the resonators in mass detection were obtained in the following order: α-graphyne > β-graphyne > 6,6,12-graphyne > γ-graphyne > graphene. The sensitivities of the resonator under different boundary conditions were also obtained. Based on the boundary conditions, the order was CCCC > SSSS > CFCF > SFSF for the considered cases. In addition, the sensitivity in mass detection decreased with an increase in resonator size. The sensitivity was the highest when the attached mass was located at the center of the resonator and gradually decreased as the mass moved away from the center.

Data Availability

The data used to support the findings of this study are included within the article.

Conflicts of Interest

The authors declare that they have no conflicts of interest.

Acknowledgments

The authors wish to thank the Ministry of Science and Technology of Taiwan for providing financial supports for this study under Projects MOST 105-2221-E-168-025 and MOST 106-2221-E-168-004.

References

[1] R. H. Baughman, H. Eckhardt, and M. Kertesz, "Structure-property predictions for new planar forms of carbon: layered phases containing sp^2 and sp atoms," *The Journal of Chemical Physics*, vol. 87, no. 11, pp. 6687–6699, 1987.

[2] A. R. Puigdollers, G. Alonso, and P. Gamallo, "First-principles study of structural, elastic and electronic properties of α-, β- and γ-graphyne," *Carbon*, vol. 96, pp. 879–887, 2016.

[3] N. V. R. Nulakani and V. Subramanian, "A theoretical study on the design, structure, and electronic properties of novel forms of graphynes," *The Journal of Physical Chemistry C*, vol. 120, no. 28, pp. 15153–15161, 2016.

[4] S. W. Cranford and M. J. Buehler, "Mechanical properties of graphyne," *Carbon*, vol. 49, no. 13, pp. 4111–4121, 2011.

[5] Q. Peng, W. Ji, and S. De, "Mechanical properties of graphyne monolayers: a first-principles study," *Physical Chemistry Chemical Physics*, vol. 14, no. 38, pp. 13385–13391, 2012.

[6] S. Ajori, R. Ansari, and M. Mirnezhad, "Mechanical properties of defective γ-graphyne using molecular dynamics simulations," *Materials Science and Engineering: A*, vol. 561, pp. 34–39, 2013.

[7] N. K. Perkgöz and C. Sevik, "Vibrational and thermodynamic properties of α-, β-, γ-, and 6, 6, 12-graphyne structures," *Nanotechnology*, vol. 25, no. 18, article 185701, 2014.

[8] R. Couto and N. Silvestre, "Finite element modelling and mechanical characterization of graphyne," *Journal of Nanomaterials*, vol. 2016, Article ID 7487049, 15 pages, 2016.

[9] J. Qu, H. Zhang, J. Li, S. Zhao, and T. Chang, "Structure-dependent mechanical properties of extended beta-graphyne," *Carbon*, vol. 120, pp. 350–357, 2017.

[10] F. C. Rodrigues, N. Silvestre, and A. M. Deus, "Nonlinear mechanical behaviour of γ-graphyne through an atomistic finite element model," *Computational Materials Science*, vol. 134, pp. 171–183, 2017.

[11] S. Bagheri, A. Shameli, M. Darvishi, and G. Fakhrpour, "Molecular investigation of water adsorption on graphene and graphyne surfaces," *Physica E: Low-dimensional Systems and Nanostructures*, vol. 90, pp. 123–130, 2017.

[12] J. M. Haile, *Molecular Dynamic Simulation*, Wiley, New York, NY, USA, 1992.

[13] T. H. Fang, Z. W. Lee, and W. J. Chang, "Molecular dynamics study of the shear strength and fracture behavior of nanoporous graphene membranes," *Current Applied Physics*, vol. 17, no. 10, pp. 1323–1328, 2017.

[14] S. Rouhi and R. Ansari, "Atomistic finite element model for axial buckling and vibration analysis of single-layered graphene sheets," *Physica E: Low-dimensional Systems and Nanostructures*, vol. 44, no. 4, pp. 764–772, 2012.

[15] C. Li and T. W. Chou, "Mass detection using carbon nanotube-based nanomechanical resonators," *Applied Physics Letters*, vol. 84, no. 25, pp. 5246–5248, 2004.

[16] A. Sakhaee-Pour, M. T. Ahmadian, and A. Vafai, "Applications of single-layered graphene sheets as mass sensors and atomistic dust detectors," *Solid State Communications*, vol. 145, no. 4, pp. 168–172, 2008.

[17] H.-L. Lee, Y.-M. Wang, Y.-C. Yang, and W.-J. Chang, "Young's modulus of nanoporous γ-graphyne membrane using an atomistic finite element model," *Solid State Communications*, vol. 280, pp. 1–5, 2018.

[18] H. L. Lee, J. C. Hsu, S. Y. Lin, and W. J. Chang, "Sensitivity analysis of single-layer graphene resonators using atomic finite element method," *Journal of Applied Physics*, vol. 114, no. 12, article 123506, 2013.